Supporting Information

Construction of "environmental-friendly" CuB_x@PU self-supporting electrode toward efficient seawater electrolysis

Yiran Zhang[a], Chengyu Fu[a], Shuo Weng[a], Haiyang Lv[a], Peng Li[a], Shengwei Deng[b], Weiju Hao[a]*

[a]University of Shanghai for Science and Technology, Shanghai 200093, P. R. China.

[b]College of Chemical Engineering, Zhejiang University of Technology, Hangzhou, Zhejiang 310014, P. R. China

**Corresponding author.*

E-mail address: wjhao@usst.edu.cn

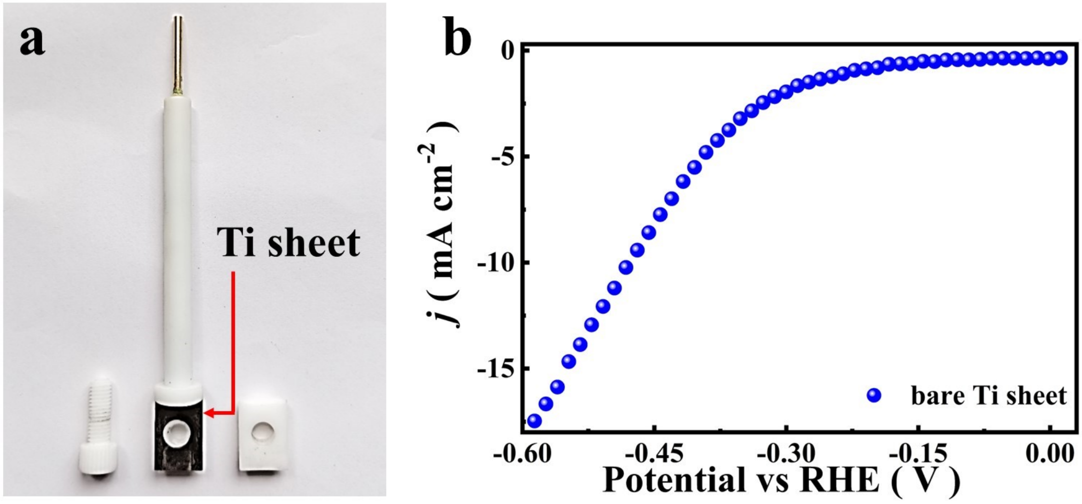

Figure S1. (a) Cutaway view of electrode holder; (b) LSV curves of bare Ti sheet.

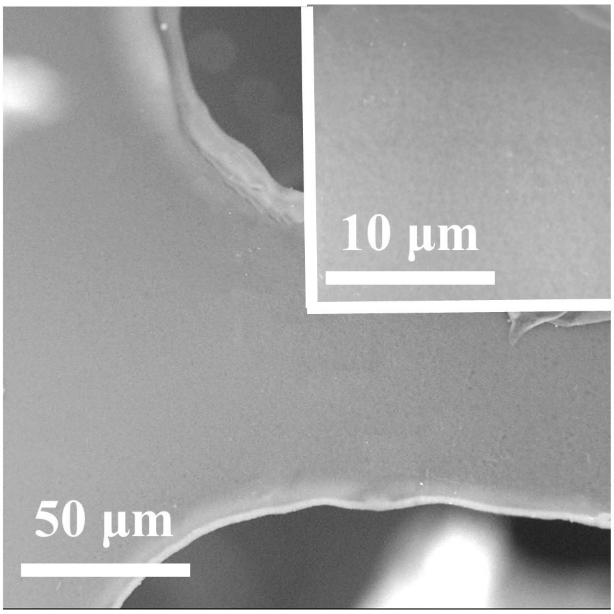

Figure S2. SEM images of bare PU substrate.

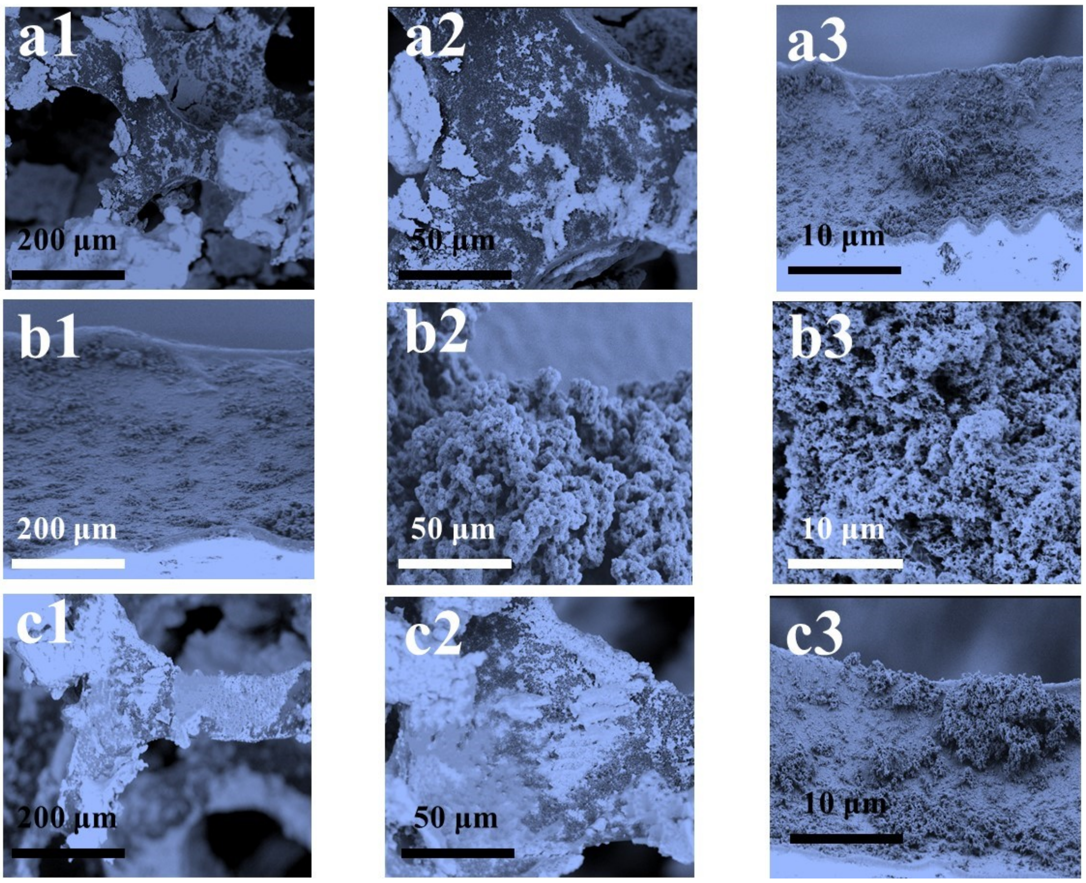

Figure S3. SEM images of CuB_x on PU substrate with different EP time: (a1, a2, a3) CuB_x@PU -30min; (b1, b2, b3) CuB_x@PU-60min; (c1, c2, c3) CuB_x@PU-90min.

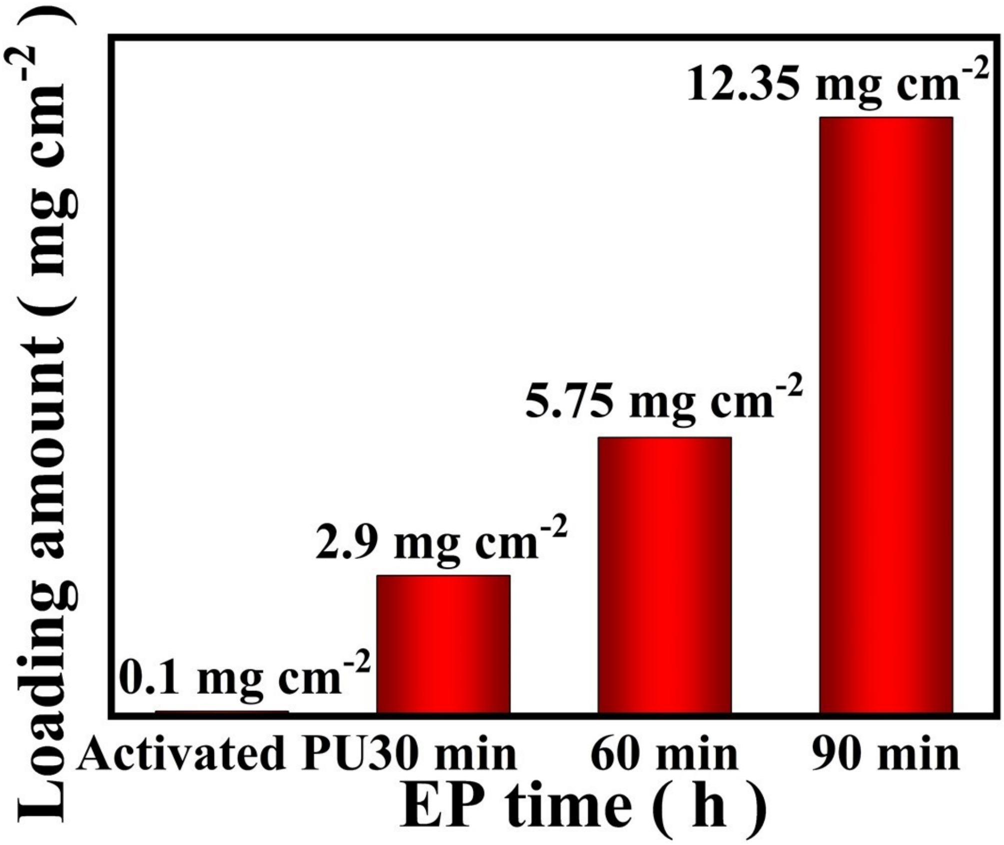

Figure S4. Loading amount of CuB_x on PU substrate with different EP time.

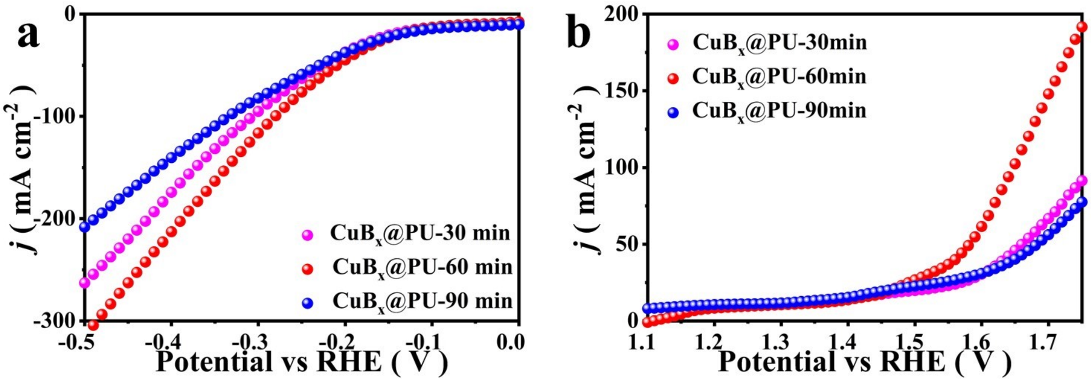

Figure S5. LSV curves of CuB_x@PU electrode with different EP time during (a) HER process and (b) OER process.

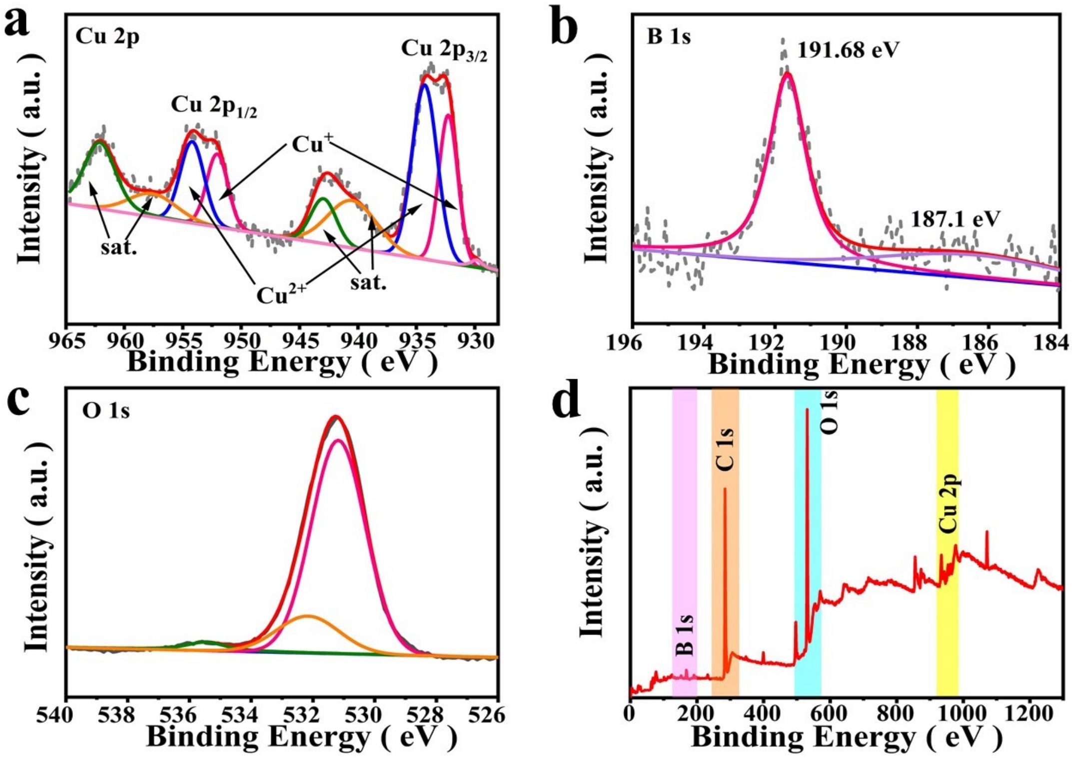

Figure S6. High-resolution XPS spectrum for CuB_x@PU electrode of (a) Cu 2p, (b) B 1s and (c) O 1s; XPS survey spectra of (d) CuB_x@PU.

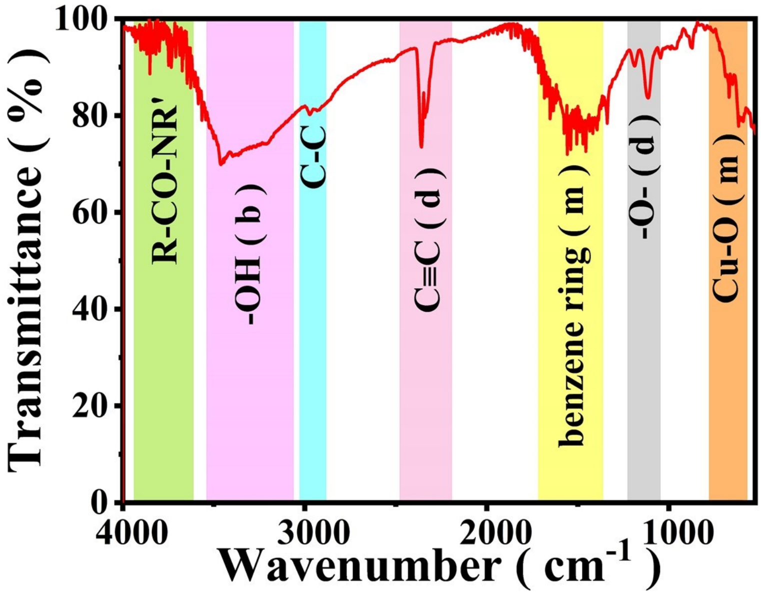

Figure S7. FT-IR spectrum of CuB_x@PU.

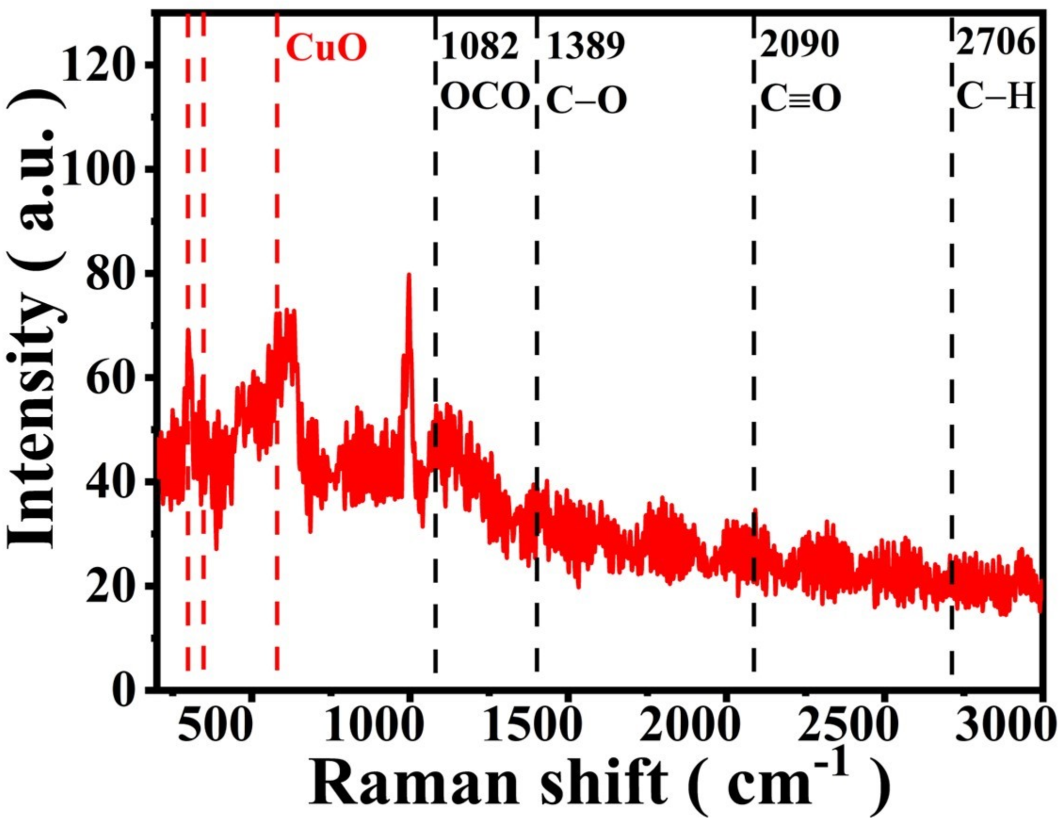

Figure S8. Raman spectrum of CuB_x@PU under 532 nm excitation.

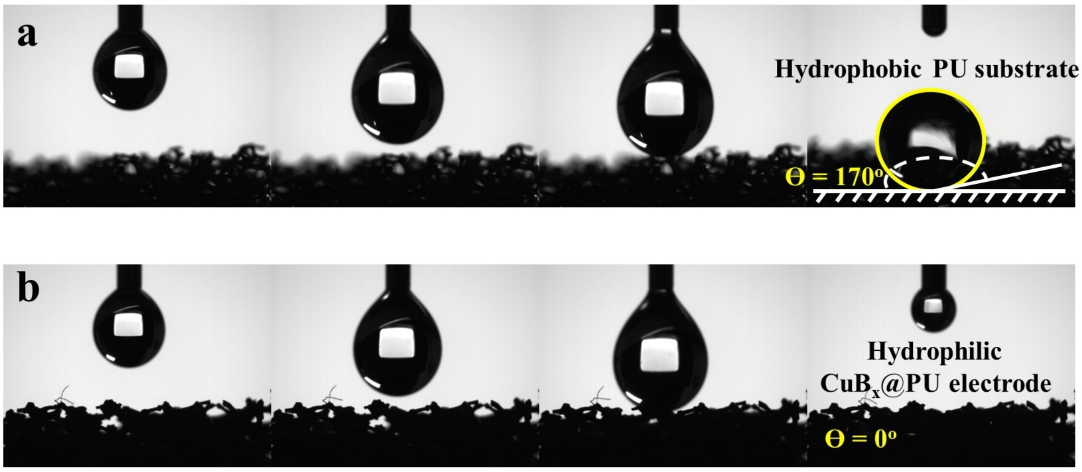

Figure S9. Contact angle measurements of (a) bare PU and (b) CuB_x@PU electrodes.

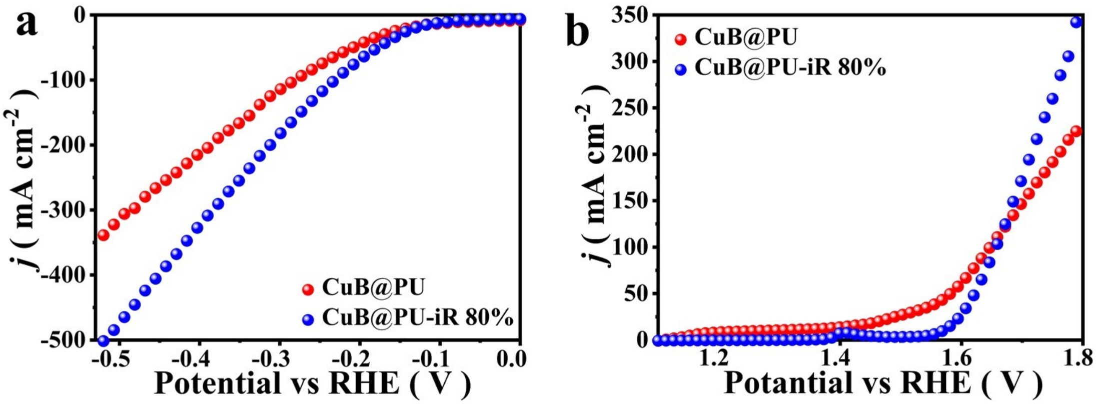

Figure S10. Comparison of LSV before and after 80% iR correction (a) HER process and (b) OER process.

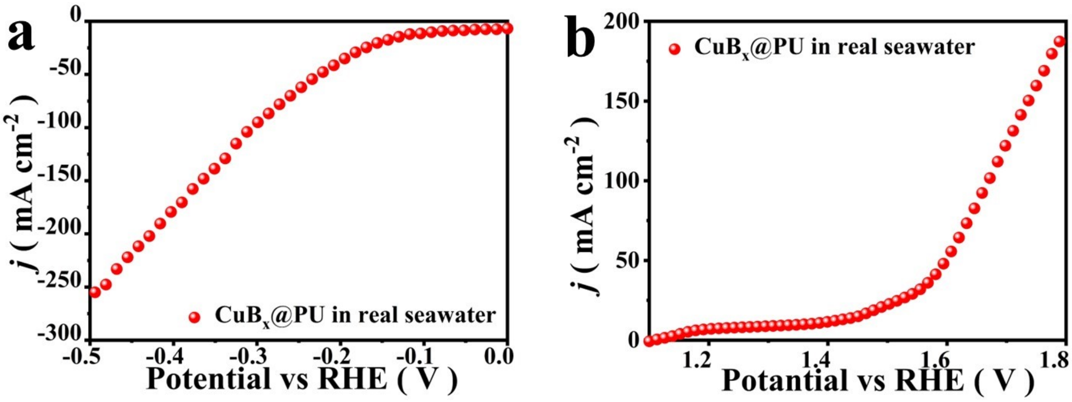

Figure S11. LSV curves of CuB_x@PU electrode in real seawater (0.5 M NaCl) during (a) HER process and (b) OER process.

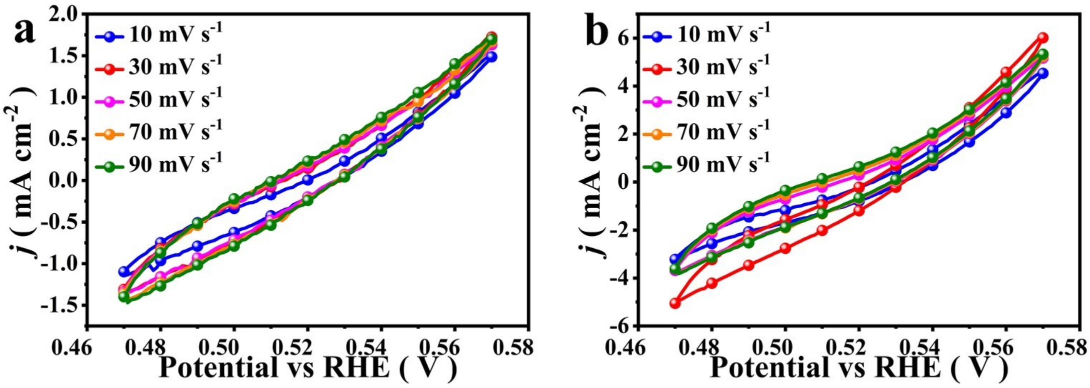

Figure S12. CV curves within a non-faradaic reaction region of 0.47 V~0.57 V verses RHE at different scan rates toward HER for (a) CuB_x@PU (b) CuB_x@NF.

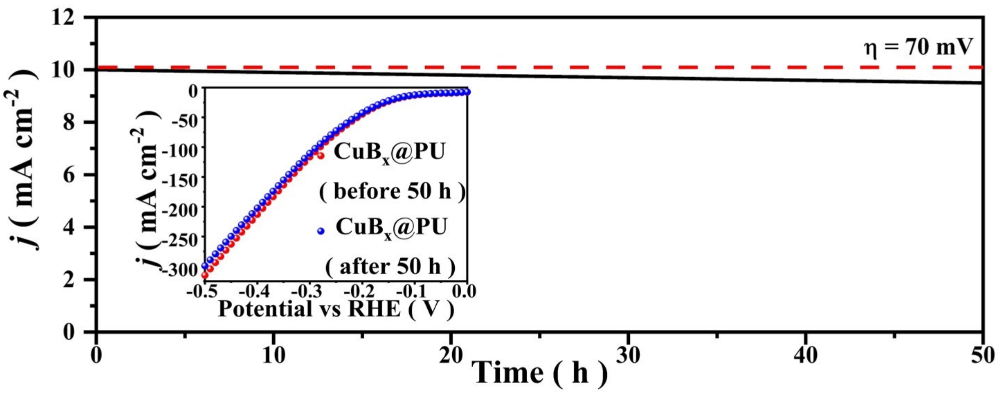

Figure S13. Chronopotentiometric measurement of HER at 70 mV. Inset: LSV curves of CuB_x@PU before and after HER cycles

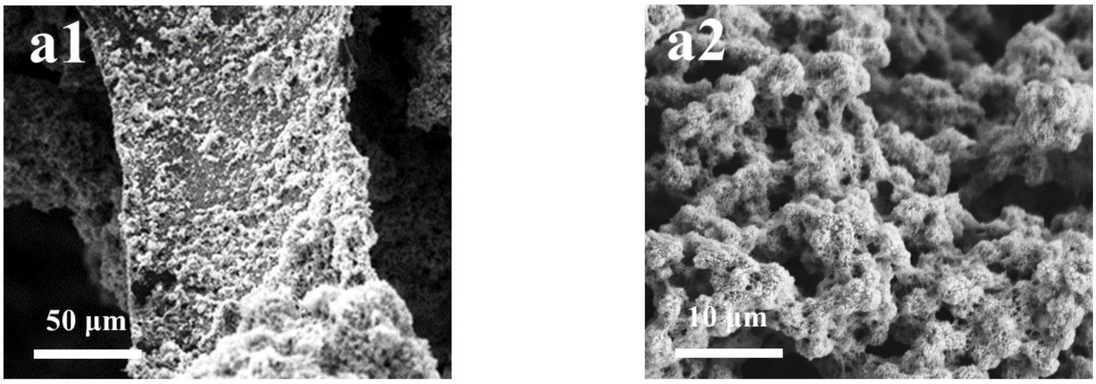

Figure S14. SEM images of (a1, a2) post-HER.

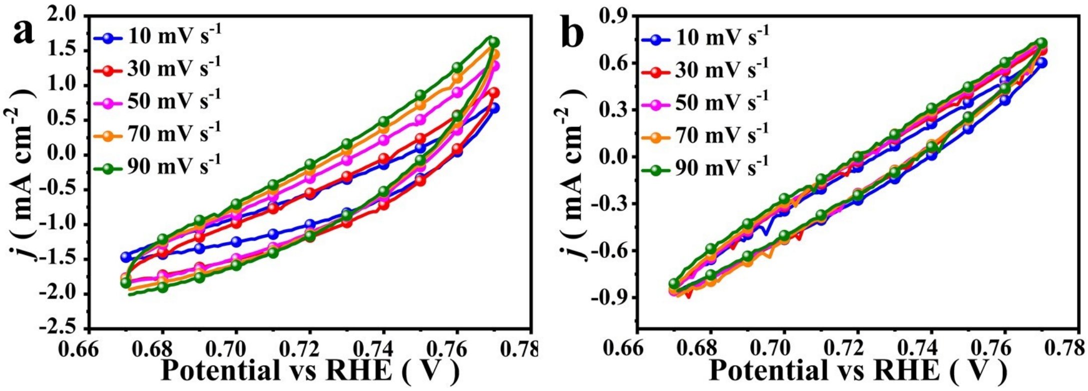

Figure S15. CV curves within a non-faradaic reaction region of 0.65 V~0.77 V verses RHE at different scan rates toward OER for (a) CuB_x@PU and (b) CuB_x@NF.

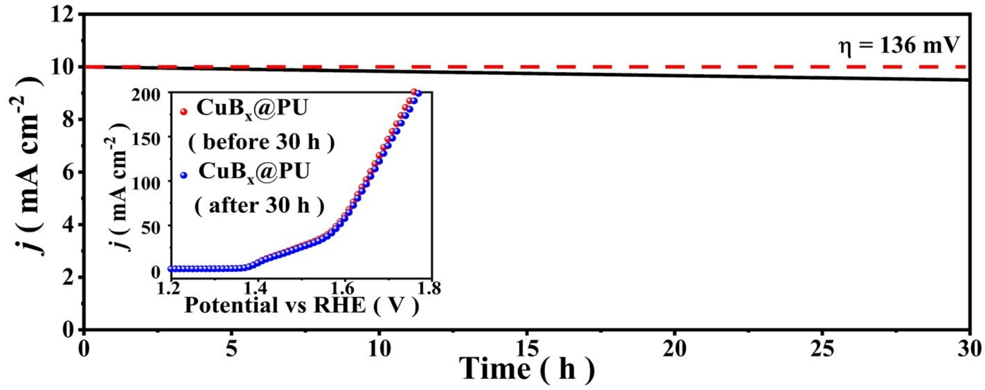

Figure S16. Chronopotentiometric measurement of OER at 136 mV. Inset: LSV curves of CuB_x@PU before and after OER cycles.

Figure S17. SEM images of (a1, a2) post-OER samples.

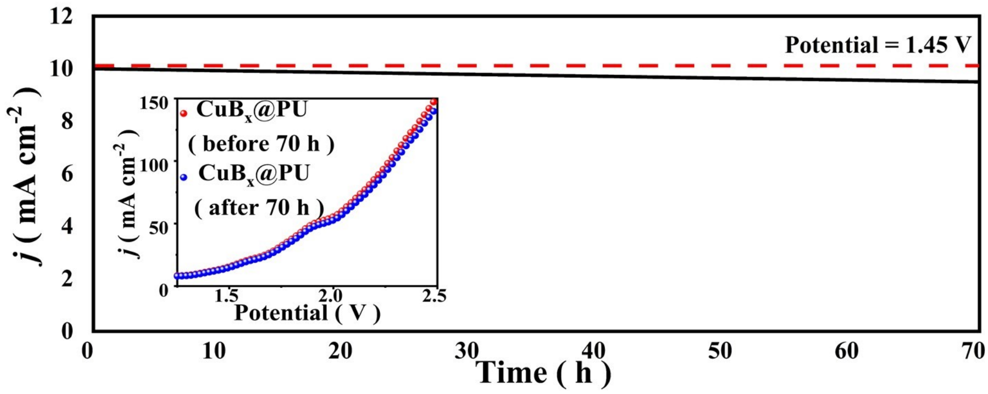

Figure S18. Chronopotentiometric measurement of the overall water splitting at the constant potential of 1.45 V. Inset: LSV curves of CuB_x@PU before and after overall water splitting.

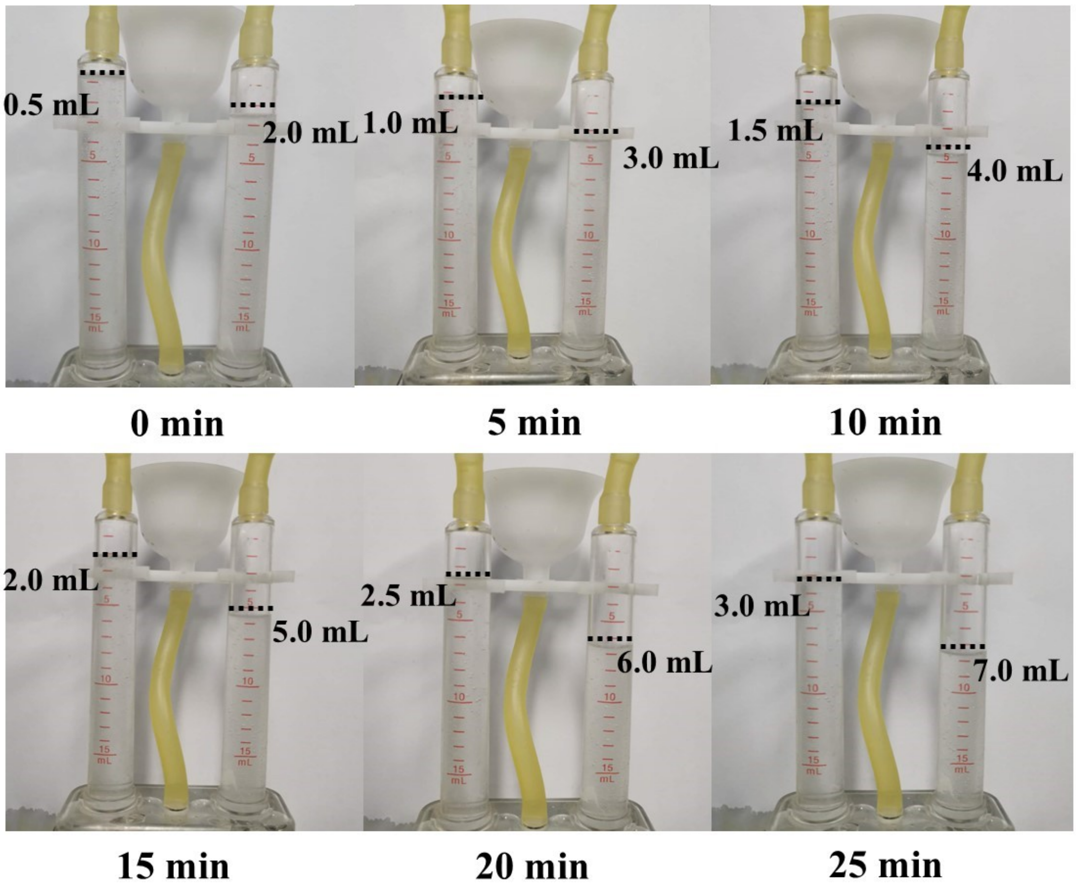

Figure S19. Photographs of H_2 and O_2 collected per five minutes at the current density of 100 mA cm^{-2}.

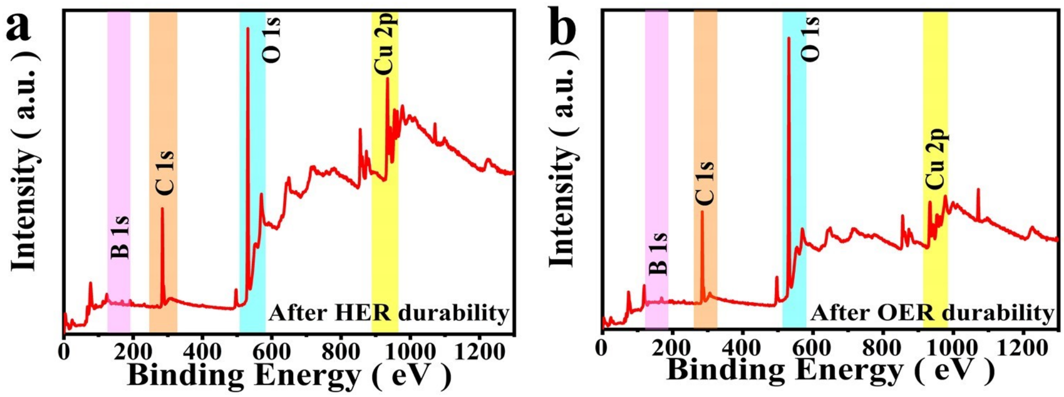

Figure S20. XPS survey spectra of (a) post-HER and (b) post-OER samples.

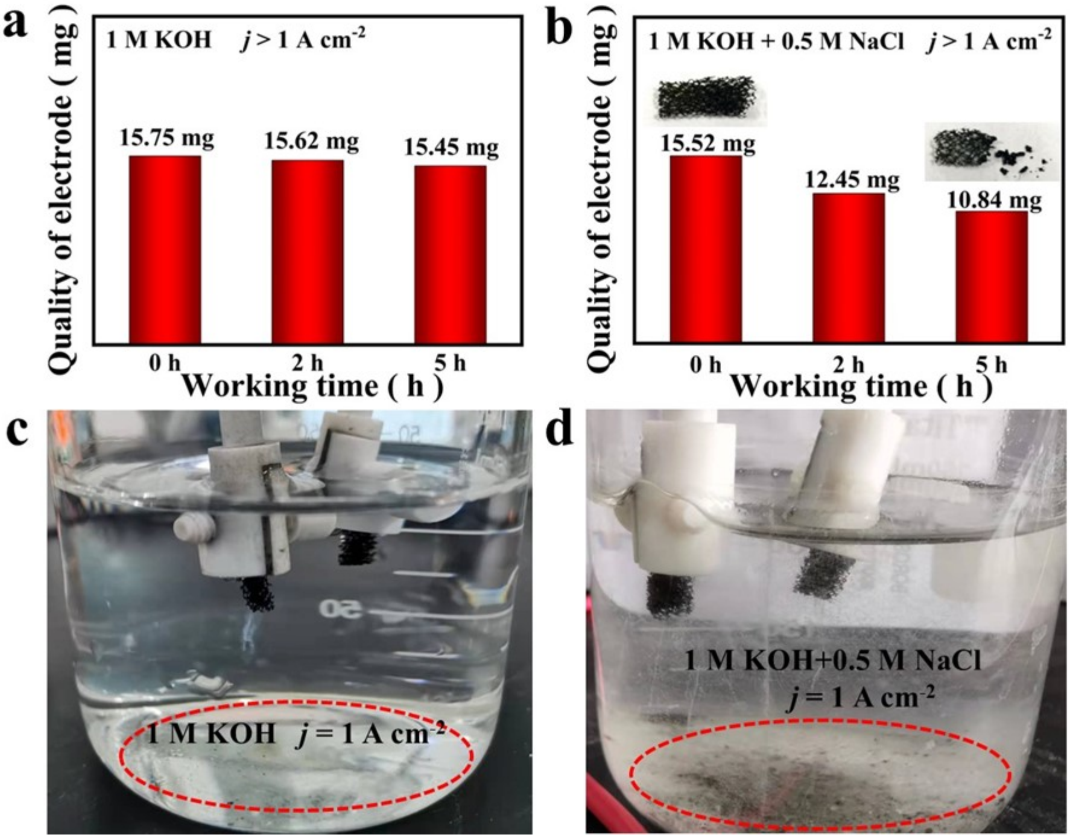

Figure S21. (a, b) Quality of CuB_x@PU with different working time at high current density (j > 1 A cm^{-2}) in the solution of 1M KOH and 1M KOH + 0.5 M NaCl; (c, d) state of 1M KOH and 1M KOH + 0.5 M NaCl electrolytes at high current density (j > 1 A cm^{-2}).

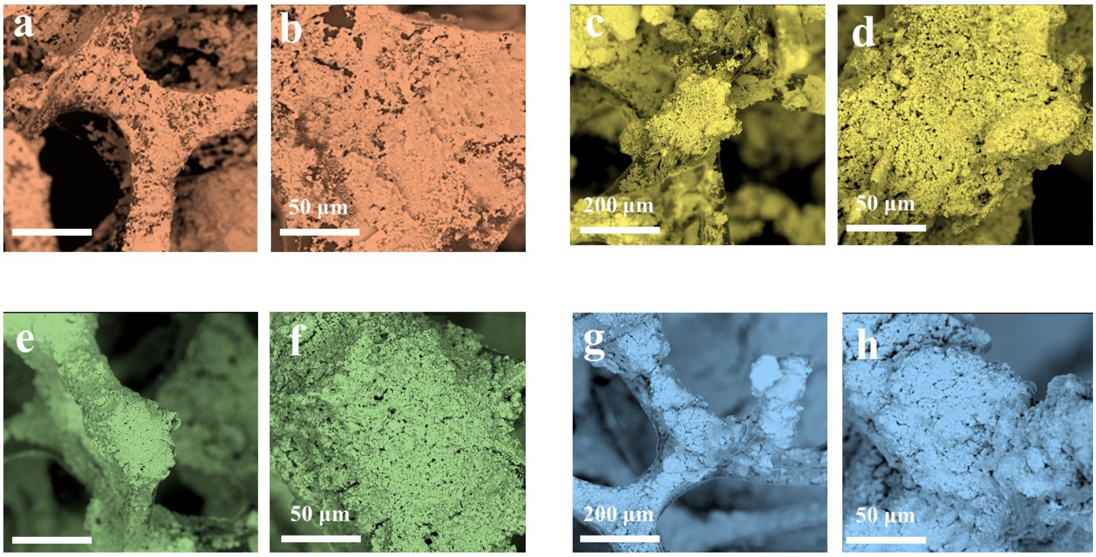

Figure S22. SEM images of (a,b) CuB-Mo@PU; (c,d) CuB-P@PU; (e,f) CuB-Ni@PU and (g,h) CuB-Co@PU.

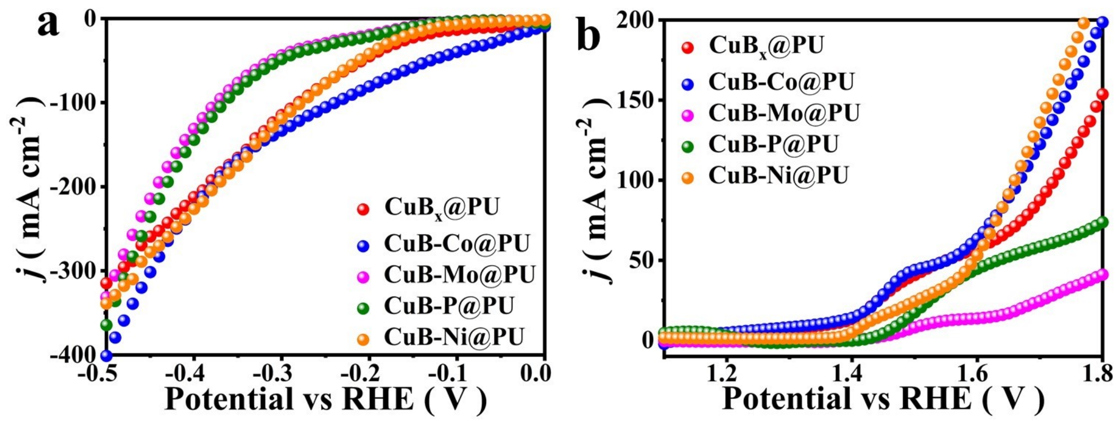

Figure S23. LSV curves of CuB_x@PU electrode doped with other (non)mentals of Co/Mo/P/Ni during (a) HER process and (b) OER process.

Supporting Tables

Table S1. ICP-AES analysis results of CuB_x-based catalytic electrodes.

Catalysts	Cu	B	Co/Mo/Ni/P	Atomic Ratio (Cu:B)
CuB_x@PU	3.23	29.80		1:9.02
post-HER	1.68	15.17		1:9.09
post-OER	1.88	20.32		1:11.1
Co-doped CuB_x@PU	1.55	24.57	5.59	1:16.7
Mo-doped CuB_x@PU	0.5	10.10	0.22	1:25.0
Ni-doped CuB_x@PU	1.98	37.86	5.22	1:20.1
P-doped CuB_x@PU	1.72	24.79	0.06	1:25.2

Table S2. Comparison of HER performance of CuB_x@PU catalyst with recently reported Cu-based catalysts under alkaline conditions.

Catalysts	Electrolyte	*j* (mA cm^{-2})	η (mV)	Loading Amount	Reference
CuB_x@PU	1.0 M KOH+0.5 M NaCl	10	70	5.75 mg cm^{-2}	This work
Ni-Mo/Cu	1.0 M KOH	20	152	2.17 mg cm^{-2}	1
Cu plate NiFeLDH	1.0 M KOH	10	116	2.2 mg cm^{-2}	2
Mo-/Co-NC/Cu	1.0 M KOH	100	71	N/A	3
Co-N-C/Cu	1.0 M KOH	100	155	N/A	3
Mo-N-C/Cu	1.0 M KOH	100	183	N/A	3
N-C/Cu	1.0 M KOH	100	21	N/A	4
RuCu NSs/C	1.0 M KOH	10	20	N/A	4
$NiCo_2O_4/Cu_xO/Cu$	1.0 M KOH	10	92	2.9 mg cm^{-2}	5
CuNi@NiFeCu	1.0 M KOH	10	42	1.95 mg cm^{-2}	6
$CuO_x@Co_3O_4$NRs/CF	1.0 M KOH	50	242	N/A	7
Pt-Cu@Cu_xO NWs	1.0 M KOH	10	72	18.9 mg cm^{-2}	8
Cu-Ni_3S_2/Co_3S_4	1.0 M KOH	10	79	N/A	9
Cu@CoS_x/CF	1.0 M KOH	10	134	3.9 mg cm^{-2}	10
Cu_3N@CoNiCHs/CF	1.0 M KOH	10	182	6.23 mg cm^{-2}	11
$CuFe_2O_4$	1.0 M KOH	10	103	1.66 mg cm^{-2}	12
Cu-Foam@CuCoNC-500	1.0 M KOH	10	59.2	N/A	13
Cu-CoP NAs/CP	1.0 M PBS	10	81	3.95 mg cm^{-2}	14

$CoNiMo_4$-21/CuOx/CF	1.0 M KOH	10	46	N/A	[15]
Fe-Ni_2P@PC/Cu_xS	1.0 M KOH	10	112.9	2.2 mg cm^{-2}	[16]
Cu-(a-$NiSe_x$/c-$NiSe_2$)/TiO_2	1.0 M KOH	10	156.9	1.5 mg cm^{-2}	[17]
Co-Cu-W	1.0 M KOH	10	100	1.25 mg cm^{-2}	[18]
$NiFeO_x$@NiCu	1.0 M KOH	10	66	0.4 mg cm^{-2}	[19]
1D-Cu@Co-CoO/Rh	1.0 M KOH+0.5 M NaCl	10	137.7	N/A	[20]
NiP_2-FeP_2 / Cu-NW / Cu-f	1.0 M KOH+0.5 M NaCl	10	23.6	N/A	[21]

Table S3. Comparison of OER performance of CuB_x@PU catalyst with recently reported Cu-based catalysts under alkaline conditions.

Catalyst	Electrolyte	*j* (mA cm^{-2})	η (mV)	Loading Amount	References
CuB_x@PU	1.0 M KOH+0.5 M NaCl	10	136	5.75 mg cm^{-2}	This work
Ni-Mo/Cu	1.0 M KOH	20	280	2.17 mg cm^{-2}	1
Cu plate NiFeLDH	1.0 M KOH	10	199	2.2 mg cm^{-2}	2
Mo-/Co-NC/Cu	1.0 M KOH	100	318	N/A	3
RuCu NSs/C	1.0 M KOH	10	234	N/A	4
$NiCo_2O_4/Cu_xO/Cu$	1.0 M KOH	10	213	2.9 mg cm^{-2}	5
CuNi@NiFeCu	1.0 M KOH	50	285	1.95 mg cm^{-2}	6
$CuO_x@Co_3O_4$NRs/CF	1.0 M KOH	50	240	N/A	7
Pt-Cu@Cu_xO NWs	1.0 M KOH	10	250	18.9 mg cm^{-2}	8
Cu-Ni_3S_2/Co_3S_4	1.0 M KOH	50	160	N/A	9
Cu@CoS_x/CF	1.0 M KOH	10	160	3.9 mg cm^{-2}	10
Cu_3N@CoNiCHs/CF	1.0 M KOH	10	155	6.23 mg cm^{-2}	11
$CuFe_2O_4$	1.0 M KOH	10	298	1.66 mg cm^{-2}	12
Cu-Foam@CuCoNC-500	1.0 M KOH	10	245	N/A	13
Cu-CoP NAs/CP	1.0 M PBS (P*BS*)	10	411	3.95 mg cm^{-2}	14
$CoNiMo_4$-21/CuOx/CF	1.0 M KOH	10	221	N/A	15
Fe-Ni_2P@PC/Cu_xS	1.0 M KOH	50	330	2.2 mg cm^{-2}	16

Cu-(a-$NiSe_x$/c-$NiSe_2$)/TiO_2	1.0 M KOH	10	339	1.5 mg cm^{-2}	[17]
Co-Cu-W	1.0 M KOH	10	300	1.25 mg cm^{-2}	[18]
$NiFeO_x$@NiCu	1.0 M KOH	10	300	0.4 mg cm^{-2}	[19]
1D-Cu@Co-CoO/Rh	1.0 M KOH+0.5 M NaCl	10	260	N/A	[20]

Table S4. Comparison of overall-water splitting performance of CuB_x@PU catalyst with recently reported Cu-based catalysts under alkaline conditions.

Catalysts	Electrolyte	*j* (mA cm^{-2})	Potential (V)	Loading Amount	Reference
CuB_x@PU	1.0 M KOH+0.5 M NaCl	10	1.45	5.75 mg cm^{-2}	This work
Ni-Mo/Cu	1.0 M KOH	20	1.69	2.17 mg cm^{-2}	[1]
Cu plate NiFeLDH	1.0 M KOH	10	1.54	2.2 mg cm^{-2}	[2]
Mo-/Co-NC/Cu	1.0 M KOH	100	1.62	N/A	[3]
RuCu NSs/C	1.0 M KOH	10	1.49	N/A	[4]
$NiCo_2O_4/Cu_xO$/Cu	1.0 M KOH	10	1.61	2.9 mg cm^{-2}	[5]
CuNi@NiFeCu	1.0 M KOH	10	1.51	1.95 mg cm^{-2}	[6]
CuO_x@Co_3O_4NRs/CF	1.0 M KOH	10	1.60	N/A	[7]
Pt-Cu@Cu_xO NWs	1.0 M KOH	10	1.56	18.9 mg cm^{-2}	[1]
Cu-Ni_3S_2/Co_3S_4	1.0 M KOH	10	1.49	N/A	[9]
Cu@CoS_x/CF	1.0 M KOH	10	1.50	3.9 mg cm^{-2}	[10]
Cu_3N@CoNiCHs/CF	1.0 M KOH	10	1.58	6.23 mg cm^{-2}	[11]
$CuFe_2O_4$	1.0 M KOH	10	1.62	1.66 mg cm^{-2}	[12]
Cu-Foam@CuCoNC-500	1.0 M KOH	10	1.52	N/A	[13]
Cu-CoP NAs/CP	1.0 M PBS (Phosphate Buffer Solution)	10	1.72	3.95 mg cm^{-2}	[14]
$CoNiMo_4$-	1.0 M KOH	50	1.53	N/A	[15]

21/CuOx/CF					
$Fe\text{-}Ni_2P@PC/Cu_xS$	1.0 M KOH	10	1.62	2.2 mg cm^{-2}	[16]
$Cu\text{-}(a\text{-}NiSe_x/c\text{-}NiSe_2)/TiO_2$	1.0 M KOH	10	1.62	1.5 mg cm^{-2}	[17]
Co-Cu-W	1.0 M KOH	10	1.80	1.25 mg cm^{-2}	[18]
$NiFeO_x@NiCu$	1.0 M KOH	10	1.67	0.4 mg cm^{-2}	[19]
1D-Cu@Co-CoO/Rh	1.0 M KOH+0.5 M NaCl	10	1.60	N/A	[20]
$NiP_2\text{-}FeP_2$ / Cu-NW / Cu-f	1.0 M KOH+0.5 M NaCl	10	1.40	N/A	[21]
Ru/Cu-doped RuO_2	1.0 M KOH	10	1.47	N/A	[22]

References

1. S. Zhao, J. Huang, Y. Liu, J. Shen, H. Wang, X. Yang, Y. Zhu and C. Li, *J Mater Chem A*, 2017, **5**, 4207-4214.
2. L. Yu, H. Zhou, J. Sun, F. Qin, F. Yu, J. Bao, Y. Yu, S. Chen and Z. Ren, *Energ Environ Sci*, 2017, **10**, 1820-1827.
3. H. Shi, T. Dai, W. Wan, Z. Wen, X. Lang and Q. Jiang, *Adv Funct Mater*, 2021, **31**, 2102285.
4. Q. Yao, B. Huang, N. Zhang, M. Sun, Q. Shao and X. Huang, *Angew Chem Int Edit*, 2019, **58**, 13983-13988.
5. Q. Ouyang, Z. Lei, Q. Li, M. Li and C. Yang, *J Mater Chem A*, 2021, **9**, 14466-14476.
6. D. Cao, H. Xu and D. Cheng, *Appl Catal B-Environ*, 2021, **298**, 120600.
7. Q. Zhou, T. Li, J. Qian, Y. Hu, F. Guo and Y. Zheng, *J Mater Chem A*, 2018, **6**, 14431-14439.
8. T. Duy Thanh, L. Huu Tuan, D. Thi Luu Luyen, N. H. Kim and J. H. Lee, *Nano Energy*, 2019, **59**, 216-228.
9. H. Su, S. Song, S. Li, Y. Gao, L. Ge, W. Song, T. Ma and J. Liu, *Appl Catal B-Environ*, 2021, **293**, 120225.
10. Y. Liu, Q. Li, R. Si, G. Li, W. Li, D. Liu, D. Wang, L. Sun, Y. Zhang and X. Zou, *Adv Mater*, 2017, **29**, 1606200.
11. S. Liu, M. Gao, S. Liu and J. Luo, *Appl Catal B-Environ*, 2021, **292**, 120148.
12. V. Sharma, U. N. Pan, T. I. Singh, A. K. Das, N. H. Kim and J. H. Lee, *Chem*

Eng J, 2021, **415**, 127779.

13. H. Sun, Q. Li, Y. Lian, C. Zhang, P. Qi, Q. Mu, H. Jin, B. Zhang, M. Chen, Z. Deng and Y. Peng, *Appl Catal B-Environ*, 2020, **263**, 118139.
14. L. Yan, B. Zhang, J. Zhu, Y. Li, P. Tsiakaras and P. K. Shen, *Appl Catal B-Environ*, 2020, **265**, 118555.
15. M. Gu, X. Deng, M. Lin, H. Wang, A. Gao, X. Huang and X. Zhang, *Adv Energy Mater*, 2021, **11**, 2102361.
16. D. T. Tran, H. T. Le, V. H. Hoa, N. H. Kim and J. H. Lee, *Nano Energy*, 2021, **84**, 105861.
17. K. R. Park, D. T. Tran, T. T. Nguyen, N. H. Kim and J. H. Lee, *Chem Eng J*, 2021, **422**, 130048.
18. D. Gao, R. Liu, J. Biskupek, U. Kaiser, Y. Song and C. Streb, *Angew Chem Int Edit*, 2019, **58**, 4644-4648.
19. Y. Zhou, Z. Wang, Z. Pan, L. Liu, J. Xi, X. Luo and Y. Shen, *Adv Mater*, 2019, **31**, 1806769.
20. T. Phan Khanh Linh, T. Duy Thanh, D. Malhotra, S. Prabhakaran, D. H. Kim, N. H. Kim and J. H. Lee, *Small*, 2021, **17**, 2103826.
21. A. Kumar, V. Q. Bui, J. Lee, A. R. Jadhav, Y. Hwang, M. G. Kim, Y. Kawazoe and H. Lee, *ACS Energy Lett*, 2021, **6**, 354-363.
22. K. Yang, P. Xu, Z. Lin, Y. Yang, P. Jiang, C. Wang, S. Liu, S. Gong, L. Hu and Q. Chen, *Small*, 2018, **14**, 1803009.